

# MHD Equilibrium and Stability of Spherical Tokamak Plasma with Current Hole

MIZUGUCHI Naoki and HAYASHI Takaya

National Institute for Fusion Science, Toki 509-5292, Japan

(Received: 9 December 2003 / Accepted: 24 February 2004)

## Abstract

The potential characteristics of spherical tokamak configurations with current hole are investigated from the point of view of magnetohydrodynamic (MHD) equilibrium and stability. The effect of the toroidal shear flows is also considered by using a modified Grad-Shafranov equation. Linear and nonlinear stability for low- $n$  kink modes and intermediate- $n$  ballooning mode is analyzed by means of numerical simulations.

## Keywords:

spherical tokamak, current hole, ballooning mode, magnetohydrodynamics

## 1. Introduction

In conventional large tokamak experiments such as JT-60U [1] and JET [2], a very good confinement, which is named the internal transport barrier (ITB), is observed. In the ITB tokamak the pressure gradient is mainly sustained in the edge region, and becomes almost flat in the core region, on the other hand. As an extreme of ITBs, an unique configuration has been observed recently. The plasma current goes to zero around the magnetic axis, and the plasma is confined at very high beta. This is named ‘current hole’. Such configurations attract a great deal of attention as a candidate of fusion core plasma, because high beta plasma confinement can be obtained with large bootstrap fraction.

In the past several years, the low-aspect-ratio, or spherical tokamak (ST) concept [3] has been studied intensively, since good confinement and stability at high beta can be obtained experimentally. Therefore, the capability of ST configurations with current hole should be examined in order to explore the reactor-sized STs in future.

In this paper, we investigate the properties of the equilibrium and the stability of STs with current hole. Furthermore, the effect of plasma shear flow due to the ITB is discussed.

## 2. Equilibria

An axisymmetric equilibrium is obtained analytically by using the Grad-Shafranov equation,

$$j_{\theta} = -\frac{1}{r} \Delta^* \psi = rp' + \frac{1}{r} FF', \quad (1)$$

where the elliptic operator  $\Delta^*$  is given by  $\Delta^* \equiv r \frac{\partial}{\partial r} \left( \frac{1}{r} \frac{\partial}{\partial r} \right) + \frac{\partial^2}{\partial z^2}$ .  $\psi$  and  $j_{\theta}$  are the magnetic flux function and the toroidal

current, respectively. Two arbitrary functions  $p$  and  $F$  are expressed that  $p = p(\psi)$  and  $F = F(\psi) = rB_{\theta}$ , where  $p$  and  $B$  are the plasma pressure and the magnetic field, respectively. By specifying  $p$  and  $F$ , the Grad-Shafranov equation can be solved under the appropriate boundary conditions. The inversion of the elliptic operator  $\Delta^*$  is carried out by means of an iterative method with keeping the value of the total current fixed.

The ST configurations with a current hole can be calculated by choosing the functions  $p$  and  $F$  as suitable forms. In the current hole, both  $p$  and  $\psi$  are flat and  $j_{\theta} = 0$ . Therefore, by setting  $p'(\psi)$  and  $F'(\psi)$  to go zero at both the magnetic axis and the edge, the current hole configurations can be modeled. We use a power of trigonometric functions for them to insure the continuity and smoothness of the quantities at the boundaries.

An example of numerical solution of (1) for parameters of ST with current hole is shown in Fig. 1. The radial profile of the pressure, the toroidal current, and the safety factor  $q$  are plotted in Fig. 1(a), and the contours of the poloidal flux are drawn in Fig. 1(b). The parameters of the equilibrium is that the aspect ratio  $A = 1.5$ , the plasma beta at the current hole  $\beta_0 = 20\%$ , and the minimum of the safety factor  $q_0 = 2.76$ .

To investigate the effect of the plasma flow on the magnetohydrodynamic (MHD) stability, we consider the equilibria, or steady state, problem of an axisymmetric tokamak with stationary shear flow. The flow considered here does not change in time, but varies in space. In this paper, we investigate a specific case that only toroidal shear flow exists. More general treatment, including poloidal component of

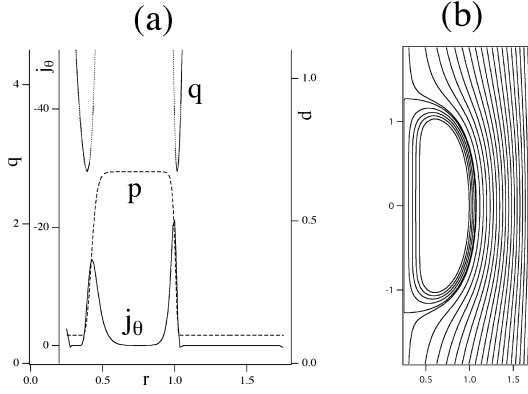


Fig. 1 Numerical equilibrium of ST with current hole. (a) radial profile of  $p$ ,  $j_\theta$  and  $q$ , (b) poloidal flux.

flow, is our future interest.

Now we start from the force balance equation of MHD fluid,

$$-\nabla p + \mathbf{j} \times \mathbf{B} - \hat{\mathbf{r}} \frac{v_\theta^2}{r} = 0 \quad (2)$$

with the centrifugal force, which is caused by the existence of the toroidal flow.

In the same manner as the derivation of the normal Grad-Shafranov equation (1), we obtain a couple of modified Grad-Shafranov equations,

$$\Delta^* \psi = -r^2 \frac{p_r}{\psi_r} - FF' - \frac{r^3 f^2}{\psi_r}, \quad (3)$$

$$\Delta^* \psi = -r^2 \frac{p_z}{\psi_z} - FF', \quad (4)$$

where the subscript of  $p$  and  $\psi$  denotes the partial derivatives. Here,  $F = rB_\theta$  and  $f = v_\theta/r$  are found to be a function of  $\psi$ , or  $F = F(\psi)$  and  $f = f(\psi)$ , however,  $p$  no longer depends on  $\psi$  alone for  $v_\theta \neq 0$ . Therefore, (3) and (4) have to be solved simultaneously for the unknown variables  $\psi$  and  $p$ , specifying arbitrary functions  $F$  and  $f$ .

To obtain more perspective form for numerical computation, (3) and (4) are rewritten as,

$$\Delta^* \psi = -r^2 \frac{p_r \psi_r + p_z \psi_z}{\psi_r^2 + \psi_z^2} - FF' - \frac{\psi_r r^3 f^2}{\psi_r^2 + \psi_z^2}, \quad (5)$$

$$p_r = -\frac{\psi_r}{r^2} (\Delta^* \psi + FF') - r f^2, \quad (6)$$

$$p_z = -\frac{\psi_z}{r^2} (\Delta^* \psi + FF'). \quad (7)$$

The numerical solution proceeds in two steps. First, (5) is solved in the same manner as the normal Grad-Shafranov equation described above with a given pressure profile. Then, the pressure profile is adjusted by using (6) and (7). For the convenience of numerical solution, we do not directly integrate the pressure gradient (6) and (7), but solve an elliptic partial equation, which is obtained by taking the divergence of (6) and (7). These two steps are mutually iterated until the converged solution  $\psi$  and  $p$  is obtained. An example of the solution is shown in Fig. 2. Here, we model the toroidal shear

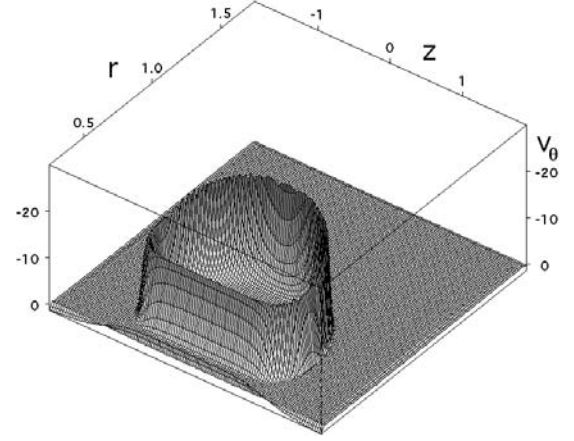


Fig. 2 Birds-eye view of flow profile in poloidal cross section.

flow to exist only in the region where the current exists. The maximum Mach number is about 0.03 for this case. All the other parameters used here are the same as the stationary case. The field variables do not differ so much from the stationary case.

### 3. Linear stability

To investigate the MHD stability of the equilibria obtained in the last section, we have executed nonlinear MHD simulations in a full toroidal geometry. The governing equation is a standard set of MHD equations,

$$\partial \rho / \partial t = -\nabla \cdot (\rho \mathbf{v}), \quad (8)$$

$$\partial (\rho \mathbf{v}) / \partial t = -\nabla \cdot (\rho \mathbf{v} \mathbf{v}) - \nabla p + \mathbf{j} \times \mathbf{B} + \mu (\nabla^2 \mathbf{v} + \frac{1}{3} \nabla (\nabla \cdot \mathbf{v})), \quad (9)$$

$$\partial \mathbf{B} / \partial t = -\nabla \times \mathbf{E}, \quad (10)$$

$$\partial p / \partial t = -\nabla \cdot (\rho \mathbf{v}) - (\gamma - 1) (p \nabla \cdot \mathbf{v} + \Phi), \quad (11)$$

where the used variables are following usual definitions,  $\mathbf{j} = \nabla \times \mathbf{B}$ , and  $\mathbf{E} = -\mathbf{v} \times \mathbf{B}$ . In numerical solution, the derivatives are expressed by using a finite difference method, and the time integration is done by the Runge-Kutta scheme.

Before executing the nonlinear simulations, linear stability is examined by using a linearized version of (8)-(11). The result shows that the equilibrium is linearly unstable for several modes.

The growth rate of the instability modes for each toroidal Fourier component is shown in Fig. 3, where  $n$  is the toroidal mode number. The growth rate is calculated from the perturbations in the magnetic energy. The higher- $n$  components are suppressed by assuming large dissipation, or affected much by the number of numerical grids. Therefore, we focus on only low- $n$  modes, and use  $128 \times 128$  numerical grids in the poloidal cross section in this paper.

In Fig. 3, the growth rate for the case with flow is plotted together. The result shows that the existence of the toroidal flow tends to make each mode more unstable. However, there are some components that is not affected by flows so much,

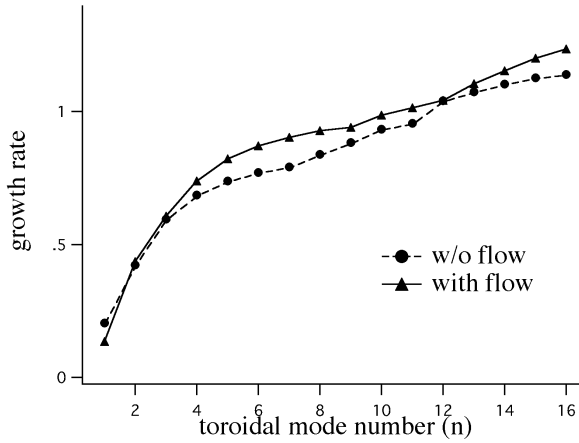


Fig. 3 Linear growth rates for each toroidal Fourier component. Solid and broken lines denote that of the case with and without flows, respectively.

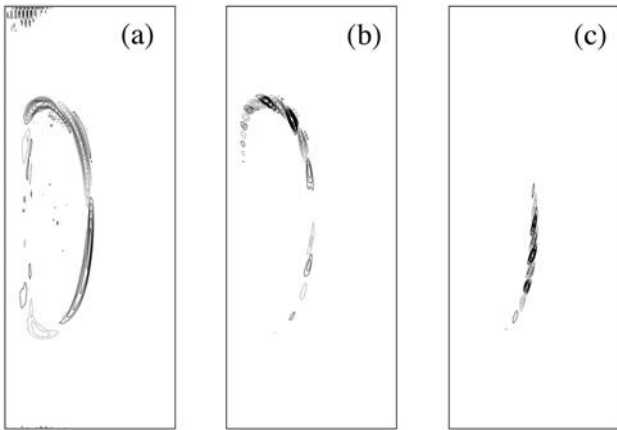


Fig. 4 Poloidal mode structures of (a)  $n = 1$ , (b) 6, and (c) 12 modes.

such as the  $n = 12$  and  $n \leq 3$  modes.

The poloidal mode structures are shown in Fig. 4 for the  $n = 1, 6$ , and 12 components. It can be seen that the dominant poloidal component of the  $n = 1$  mode is  $m = 3$ , where  $m$  is the poloidal mode number. Analysis of the driving source of the instabilities by using the energy principle shows that this 3/1 mode is a kind of current-driven (kink) instabilities. Another feature of Fig. 4 is that the structures of the higher- $n$  modes are localized poloidally, which implies that these modes are categorized into the ballooning mode.

#### 4. Non-linear simulation

To investigate further the overall dynamics of plasma, it is necessary to execute nonlinear simulations by solving directly (8)-(11). We use a finer numerical mesh with  $256 \times 256$  grids in poloidal cross section, and 64 grids in toroidal direction, to follow the mode couplings among as many modes as possible. A low-pass filtering technique is applied to remove high-wavenumber components. Since the initial flow causes no qualitative change in the linear instabilities,

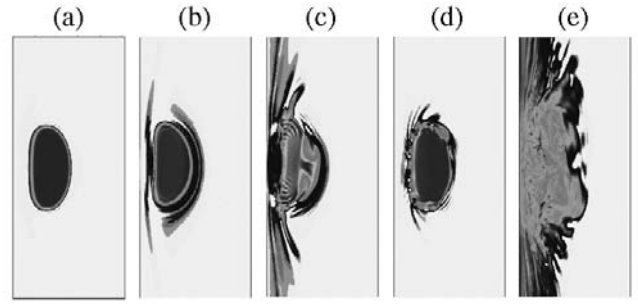


Fig. 5 Nonlinear time development of pressure profile. (a)  $t = 0$ , (b)  $t = 500$ ,  $n = 1$ , (c)  $t = 620$ ,  $n = 1$ , (d)  $t = 60$ ,  $n = 6$ , (e)  $t = 320$ ,  $n = 6$  (The time  $t$  is normalized by the Alfvén transit time.)

nonlinear simulation is done only for the case  $v_\theta = 0$  as the initial condition.

Figure 5 shows the temporal changes in the poloidal pressure profile. Simulations are executed for two eigenmodes, the  $n = 1$  (Fig. 5(b)-(c)) and the  $n = 6$  (Fig. 5(d)-(e)) modes. One can see that for both cases the shape of the cross section varies reflecting the poloidal mode structures of the linear eigenmode in the beginning ((b) and (d)), but a lot of smaller scale components appear as a result of the nonlinear couplings. The configuration goes into turbulent and destroyed in the end ((c) and (e)). So far as we can see from this result, there are no indications that the toroidal confinement recovers after that, which can be seen in our previous simulations for conventional STs without current hole [4-5]. However, it is necessary to survey simulation parameters in wider range for better understanding of the nonlinear behavior.

#### 5. Summary and discussion

The MHD equilibria of ST configurations with a current hole have been obtained numerically by solving the modified Grad-Shafranov equation. We have also obtained both equilibria with and without steady toroidal shear flows.

Linear and nonlinear MHD simulations have been executed for such equilibria. The linear results show the growth of the 3/1 kink mode and the higher- $n$  ballooning modes. The steady toroidal flows make the higher- $n$  modes more unstable. It is considered that the destabilization is caused by the centrifugal force. In our calculations, the plasma pressure profiles tend to be shifted outward under the existence of toroidal flows, so that the pressure gradient is more steepened in the low field side.

The preliminary nonlinear simulation result for the case with no toroidal flows in the initial state shows that a hard disruption of the configuration occurs. In our previous simulation result for the internal  $n = 1$  relaxation of a conventional ST plasma [5], the torus configuration recovers spontaneously through a closed vortex flow inside the  $q = 1$  surface. Another previous result for the internal reconnection event [4] also shows a spontaneous recovery of the

configuration through the magnetic reconnection process between the internal and external magnetic field. These previous results seem to imply that STs have good 'resilience'. However, the nonlinear result in this paper shows an opposite example. One of the reasons for the discrepancy might be the existence of the current hole. Because there are no MHD force balances in the current hole region to sustain the high beta plasma, the restrictive forces against the deformations would be small. However, more detailed nonlinear analysis is our ongoing subject.

The authors would like to thank Dr. Y. Ono, Dr. Y. Nagayama, Dr. M. Furukawa and Dr. H. Miura for their fruitful comments.

### References

- [1] T. Fujita *et al.*, Phys. Rev. Lett. **87**, 245001 (2001).
- [2] N.C. Hawkes *et al.*, Phys. Rev. Lett. **87**, 115001 (2001).
- [3] A. Sykes, Plasma Phys. Control. Fusion **34**, 1925 (1992).
- [4] N. Mizuguchi *et al.*, Phys. Plasmas **7**, 940 (2000).
- [5] T. Hayashi *et al.*, Nucl. Fusion **40**, 721 (2000).